J Appl Electrochem (2009) 39:147–154
DOI 10.1007/s10800-008-9648-6

ORIGINAL PAPER

Synthesis of pyridine derivatives and their influence as additives on the photocurrent of dye-sensitized solar cells

Xiong Yin · Weiwei Tan · Jingbo Zhang · Yuan Lin · Xurui Xiao · Xiaowen Zhou · Xueping Li · Babasaheb Raghunath Sankapal

Received: 29 November 2007 / Accepted: 23 July 2008 / Published online: 19 August 2008

Abstract New kinds of additive, 4-alkyloxypyridne derivatives, were synthesized by introducing an alkyloxy group into the 4-position of 2-methylpyridine. The influence of these electrolyte additives on the short-circuit photocurrent (J_{sc}) of dye sensitized solar cells was investigated by combining electrochemical and spectral techniques. With the addition of pyridine derivatives to the electrolyte, a decrease in the rate of dye regeneration was observed by laser flash photolysis measurements and cyclic voltammetry, whereas, measurement of electrochemical impedence spectra showed an increase in the charge transfer resistance due to the formation of a complex between the pyridine derivatives and iodine, as identified by an absorption peak around 378 nm in the UV–Vis spectra. This leads to a decrease in J_{sc} of dye-sensitized solar cells. This adverse effect on the J_{sc} can be attributed to reaction or coordination between the dye cations and the iodine in the electrolyte.

X. Yin · W. Tan · J. Zhang (✉) · Y. Lin (✉) · X. Xiao · X. Zhou · X. Li
Key Laboratory of Photochemistry, Beijing National Laboratory for Molecular Sciences (BNLMS), Institute of Chemistry, Chinese Academy of Sciences, Beijing 100190, China
e-mail: jbzhang@iccas.ac.cn

Y. Lin
e-mail: linyuan@iccas.ac.cn

X. Yin · W. Tan
Graduate School of Chinese Academy of Sciences, Beijing 100039, China

B. R. Sankapal
Thin Film and Nano Science Laboratory, Department of Physics, North Maharashtra University, Jalgaon 425001, India

Keywords Dye sensitized solar cell · Pyridine derivatives · Charge transfer complex · Cyclic voltammetry · Laser flash photolysis

1 Introduction

The dye sensitized nanocrystalline TiO_2 solar cell (DSSC) is a potential low-cost alternative to the conventional silicon solar cell due to its attractive features of high energy conversion efficiency and low production cost [1–3]. The typical cell consists of a nanocrystalline mesoporous TiO_2 thin film coated on conducting glass substrate with a monolayer of dye as a sensitizer, electrolyte containing iodide/triiodide and a platinum as a counter electrode. The power conversion efficiency strongly depends on the processes of electron transfer at the TiO_2/dye/electrolyte interfaces, ion diffusion within the electrolyte and redox charge transfer at the counter electrode. In particular, the electron transfer dynamics at the TiO_2/dye/electrolyte interfaces is a key factor affecting the efficiencies due to two critical parameters: short circuit photocurrent (J_{sc}) and open circuit photovoltage (V_{oc}) [4]. To the best of our knowledge, there are three different strategies to optimize these dynamic processes: (1) depositing a thin barrier of metal oxide on the TiO_2 surface to retard the charge recombination, (2) building a hydrophobic spacer between the TiO_2 and the electrolyte to reduce the back electron transfer, and (3) adding organic molecular additives to the electrolyte to shift the band edge of TiO_2. As far as the last process is concerned, several groups have investigated the potential use of additives to improve the device efficiency by means of different experimental techniques. Schlichthörl et al. have investigated the band edge movement of TiO_2 with 4-*tert*-pyridine added into the electrolyte using

intensity modulated photovoltage spectroscopy [5]. Hong et al. employed a spectroelectrochemical technique and an absorption spectrophotometry to explain the reason for improvement of V_{oc} and J_{sc} after polypyrrole anchoring on the TiO_2 thin film [6]. Neal et al. demonstrated the effect of a coadsorbent, chenodeoxycholate, on the performance of DSSCs using infrared transmittance measurements [7]. Nakade et al. measured the electron diffusion coefficient in the TiO_2 thin film with or without 4-*tert*-pyridine using laser-induced current transient measurements [8]. Zhang et al. studied the collective effect of ω-Guanidinoalkyl acid with dye Z-907 by adopting photovoltage transient spectroscopy [9]. Furthermore, with the aid of density functional calculation theory, Kusama and Sugihara investigated the interaction between iodine and several nitrogen-contained heterocyclic compounds and revealed that the efficiency is related to charge transfer complexes between heterocyclic group and iodine [10]. Cyclic voltammetry analysis, electrochemical impedance spectra (EIS) and time-resolved mid-infrared absorption spectroscopy [11, 12] were also applied to study the electron transfer dynamics at the TiO_2/dye/electrolyte interfaces.

Recently, we have studied the effects of different pyridine derivatives as additives on DSSC performance and reported that the addition of pyridine derivatives caused an increase in the photovoltage [12]. The mechanism was interpreted as a combination of surface activation and a shift of the TiO_2 conduction band edge to more negative potentials. It was found that the negative shift of the conduction band of TiO_2 was a predominant factor in improving V_{oc} of DSSCs. There have been many reports on the effects of additives on V_{oc} [5–7, 10–12], but few about their effects on J_{sc} [6, 8].

In this study an attempt has been made towards a synthetic route for a novel type of additives, 4-alkyloxypyridne derivatives. Furthermore, the use of these additives and their influence on J_{sc} of DSSCs has been discussed with the aid of transient absorption, electrochemical and impedance measurements.

2 Experimental

2.1 Materials and general methods

2-Methylpyridine, 4-*tert*-pyridine (TBP) and 3-methoxypropionitrile (MPN) were purchased from Aldrich and distilled under vacuum prior to the use. Lithium iodide (Aldrich) and iodine (Aldrich) were used without further purification. Blank electrolyte used in all experiments was a mixture of 0.5 mol L^{-1} LiI and 0.05 mol L^{-1} I_2 in MPN. All chemicals used in the synthesis were of analytical grade. All solvents were purified and dried according to the standard methods.

^{1}H NMR spectra were measured on a Bruker AMX-400 NMR spectrometer with $CDCl_3$ as solvent and tetramethylsilane (TMS) as the internal standard. Infrared spectra were recorded using the KBr pellets method on a Bruker Tensor 27 FT-IR spectrophotometer. Elemental analysis was conducted on a Thermo-Quest, CE instrument (Italy). Mass spectra were measured on a GCT-MS spectrometer, Micromass (UK). All UV–Vis absorption spectrum measurements were carried out on a Hitachi U-3010 spectrophotometer within the wavelength range 280–800 nm using MPN as a blank at room temperature.

2.2 Preparation of dye sensitized TiO_2 film

Nanocrystalline TiO_2 thin films were fabricated on fluorine doped tin oxide coated glass substrates (FTO, $\sim$20 Ω square^{-1}), as described by Grätzel and coworkers [1, 2]. A colloidal TiO_2 suspension was prepared by hydrolysis of titanium isopropoxide precursor in aqueous solution (pH = 2) under vigorous stirring at 80 °C. The suspension was then autoclaved at 250 °C for 12 h and evaporated in a rotary evaporator. The TiO_2 suspension was deposited onto FTO using the 'doctor blade' method. After drying at room temperature, the TiO_2 thin film was sintered at 450 °C for 30 min in air to form a nanocrystalline porous thin film. The film thickness is 15 μm determined using cross sectional FE-SEM [12]. The film was sensitized by immersion in an absolute ethanolic solution of 5×10^{-4} mol L^{-1} $Ru(dcbpy)_2(NCS)_2$(dcbpy: 2,2′-bipyridine4,4′-dicarboxylic acid) (N3, Solaronix) for 12 h.

2.3 Photoelectrochemical and electrochemical measurements

A two electrode sandwich cell consisting of a dye sensitized TiO_2 electrode, an organic electrolyte containing triiodide and iodine and a platinum coated FTO as a counter electrode (CE) was used for the photovoltaic measurements. The CE was prepared by thermal decomposition of 5×10^{-3} mol L^{-1} H_2PtCl_6 in 2-propanol on FTO at 390 °C for 15 min [13]. The CE and dye sensitized TiO_2 electrodes were clamped firmly together and the electrolyte was introduced to the cell by capillary action. The cell was illuminated through the dye sensitized TiO_2 thin film with active area of 0.2 cm^2. The photovoltaic performances of DSSCs were recorded with a PAR potentiostat (Model 273). A 300 W Xe arc lamp (Oriel) together with optical filters was used as a light source for simulating the solar spectrum at AM 1.5 (100 mW cm^{-2}).

Cyclic voltammetry measurements were carried out on a Solartron SI1287 electrochemical interface at a scanning rate of 50 mV s^{-1} [14]. A dye coated FTO was prepared by heating the conductive glass substrate at 120 °C for 1 h and

then immersing in 5×10^{-4} mol L^{-1} N3 ethanolic solution for 12 h. A three electrode electrochemical cell was made consisting of a dye coated FTO as working electrode (WE) and a platinized FTO conductive glass with its conductive surface split into two parts, one as CE and the other as reference electrode (RE).

Electrochemical impedance spectroscopy (EIS) was performed using a Solartron 1255B frequency response analyzer and a Solartron SI 1287 electrochemical interface system at zero bias under the frequency range 0.05–1 MHz in a symmetrical thin layer cell, which consisted of two identical platinized FTO and a Surlyn film of thickness 40 μm as the spacer [15]. The active area of the electrode was 0.25 cm^2.

2.4 Transient absorption spectroscopy (laser flash photolysis)

Flash photolysis experiments were performed immediately after placing a drop of electrolyte containing different pyridine derivatives between a fresh dye sensitized TiO_2 film and a thin microscope cover glass [16]. A transient absorption experiment with excitation light by the use of the second harmonic of a nanosecond Nd:YAG laser (continuum, 532 nm, 7 ns FWHM) was carried out in the nanosecond to microsecond range. The laser beam was initially filtered by an aperture to get a nearly homogeneous light spot with energy of 0.3 mJ $pulse^{-1}$. A pulsed Xenon arc lamp was used to provide the detecting light. The monitoring wavelength was selected using a monochromator, typically set at 800 nm, which primarily results from N3 cation absorption. The two beams were intersected vertically at the sample with its surface being kept at 45° to the excitation and detecting lights. The signals were detected by an Edinburgh Lp900 and recorded on a Tektronix TDS 3012B oscilloscope and computer.

2.5 Synthesis of 4-alkyloxy-2-methylpyridine derivatives

4-Alkyoxy-2-methylpyridine derivatives were synthesized from 2-methylpyridine according to the methodology outlined in Scheme 1. The compounds *2* [17], *3* [18], *4* [19] were prepared according to literature procedures. The products *5a*, *5b* and *5c* were synthesized from *4* according to the following steps.

2.5.1 Synthesis of product 5a (4-ethoxy-2-methylpyridine, EOP)

A solution of PCl_3 (4.56 mL, 0.05 mol) in $CHCl_3$ (10 mL) was added dropwise into a solution of *4a* (1.53 g, 0.01 mol) in $CHCl_3$ (10 mL) with ice-water cooling under

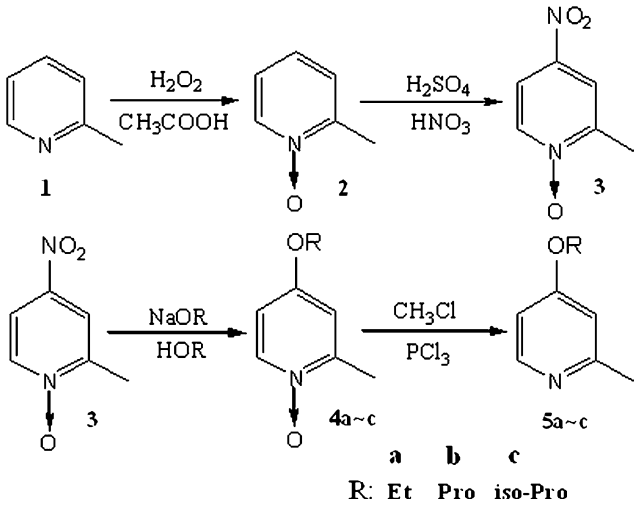

Scheme 1 The synthesis route of pyridine derivatives

N_2 atmosphere. After the addition, the solution was stirred at room temperature for 1 h and refluxed at 60 °C for another 2 h, then poured into crushed ice and neutralized with 10% NaOH solution. The organic phase was separated and the aqueous phase was further extracted with $CHCl_3$ (30 mL × 3). The combined extract was washed with brine, dried with anhydrous $NaSO_4$ and organic solvent was evaporated. The residue was isolated by chromatography on silica gel with EtOH–CH_2Cl_2 (5/95, V/V) to give the product *5a* (1.0 g) as a light yellow liquid (75%, yield). R_f: 0.28. ^{1}H NMR: 8.35 (1H, d), 6.71 (1H, d), 6.68 (1H, dd), 4.12 (2H, dd), 2.56 (3H, s), 1.48 (3H, t); MS (EI, 70 eV) (m/z) 137 (M^+, 90), 109 (100); IR (cm^{-1}, KBr): 1012, 1242; Anal. Calc. for $C_8H_{11}NO$: C, 70.04; H, 8.08; N, 10.21. Found: C, 69.89; H, 8.21; N, 10.26.

2.5.2 Synthesis of product 5b (2-methyl-4-n-propoxypyridine, POP)

The product *5b* was synthesized in a same manner as described above by reacting *4b* (0.01 mol) and PCl_3 (0.05 mol). The product *5b* was purified by column chromatography on silica gel with EtOH–CH_2Cl_2 (5/95, V/V) to give a yellow liquid (1.38 g, 92%). R_f: 0.25. ^{1}H NMR: 8.30 (1H, d), 6.66 (1H, d), 6.62 (1H, dd), 3.95 (2H, t), 2.50 (3H, s), 1.80 (2H, hexa), 1.03 (3H, t); MS (EI, 70 eV) (m/z) 151 (M^+, 48), 109 (100); IR (cm^{-1}, KBr): 1015, 1237; Anal. Calc. for $C_9H_{13}NO$: C, 71.49; H, 8.69; N, 9.26. Found: C, 71.25; H, 8.64; N, 9.28.

2.5.3 Synthesis of product 5c (2-methyl-4-iso-propoxypyridine, isoPOP)

The procedure was same as that used for *5a* and *5b* to synthesize the product *5c*. From 1.67 g (0.01 mol) of *4c*

and 0.05 mol of PCl_3 in $CHCl_3$, 1.3 g of *5c* (86% yield) as a brown liquid was obtained after column chromatography on silica gel with EtOH–CH_2Cl_2 (5/95, V/V). R_f: 0.24. ^1H NMR: 8.29 (1H, d), 6.63 (1H, d), 6.59 (1H, dd), 4.62 (1H, hepta), 2.49 (3H, s), 1.36 (6H, d); MS (EI, 70 eV) (m/z) 151(M^+, 40), 109 (100); IR (cm^{-1}, KBr): 1013, 1257; Anal. Calc. for $C_9H_{13}NO$: C, 71.49; H, 8.69; N, 9.26. Found: C, 71.38; H, 8.71; N, 9.24.

3 Results and discussion

3.1 Transient absorption for pyridine derivatives in the electrolyte

Figure 1 shows the change in the transient absorbance due to the application of a 532 nm laser pulse on a N3 sensitized TiO_2 thin film in blank electrolyte with different pyridine derivatives (0.1 mol L^{-1}). In all cases the excited N3 cations are reduced by charge recombination with electrons occupying conduction band or trap states of the TiO_2 or by iodide ions in the electrolyte. Nogueira et al. [20] reported that the decay of photoinduced absorption at 800 nm is biphasic. The fast phase is assigned to the decay of dye cations, whereas the slow phase is assigned to the decay of I_2^- radicals. Also, they have reported that the time needed to reach half of the initial absorbance ($\tau_{1/2}$) of the fast phase is in the range of microsecond. In our experiments, the decay should be assigned to the decay of dye cations only since the probed time range is in the region of a microsecond and the induced absorption signal decay is mono exponential behavior. Therefore, we applied the mono exponential equation to fit the decay curves. In the absence

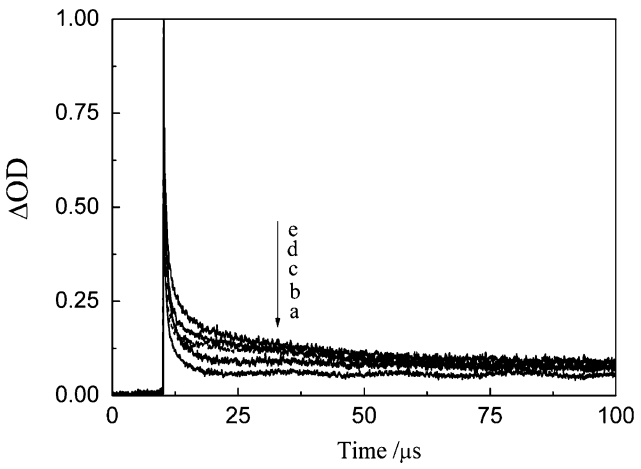

Fig. 1 Transient absorbance spectra measured at 800 nm for N3-sensitized TiO_2 thin films in blank electrolyte without (a) and with 0.1 mol L^{-1} different additives (TBP (b), POP (c), EOP (d), *iso*POP (e)). Here $\Delta OD = \log (I_{out}/I_{in})$, I_{out} and I_{in} are the output and incident optical intensities

Table 1 $\tau_{1/2}$ of dye cation of the dye sensitized TiO_2 thin film in different electrolytes shown in Fig. 2

Additive	Blank	TBP	POP	EOP	*iso*/POP
$\tau_{1/2}$/(μs)	11.08	11.99	12.35	12.71	16.35

of any derivatives (trace a), $\tau_{1/2}$ is 11.08 μs. Traces b, c, d and e were recorded after addition of TBP, POP, EOP and *iso*POP, respectively. Obviously, the addition of these pyridine derivatives to the electrolyte in all cases leads to a blocking of the dye cation reduction. Consequently, the kinetics of dye cation reduction becomes dependent on the added derivatives. In the presence of TBP, POP, EOP and *iso*POP, their half time is listed in Table 1. POP and EOP show nearly the same effect on the dye cation reduction. The reduced rate of dye cation decreased in the following order: Blank > TBP > POP > EOP > *iso*POP.

3.2 Cyclic voltammetry for pyridine derivatives in the electrolyte

The influence of pyridine derivatives on the kinetics between the oxidized dye cation and iodide in the electrolyte was studied by cyclic voltammetry (*CV*) measurements. Figure 2a shows the *CV* curves of a dye coated FTO electrode in the blank electrolyte with different concentrations of POP. In the *CV* measurements, the potential is referred to the equilibrium potential (E_{eq}) of the iodide/triiodide couple. The anodic peak is not observed for the bare FTO electrode (not shown in Fig. 2a), which is assigned to anodic oxidization of iodide by the oxidized dye. The anodic peak potential shifts positively and the peak current density gradually decreases when the concentration of POP in the electrolyte is increased from 0.1 to 1.0 mol L^{-1}. Figure 2b shows the *CV* curves of a dye coated FTO electrode in blank electrolyte with 0.1 mol L^{-1} different derivatives. The anodic peak current density decreases in the following order: Blank > TBP > POP > EOP > *iso*POP, whereas the peak potential increases as: Blank < TBP < POP < EOP < *iso*POP. The cathodic peak is absent in this scanning range indicating the irreversible behavior of this electrochemical reaction at a dye coated FTO electrode. In order to further analyze the reason for the shift of anodic peak potential, we applied the ultra microelectrode technique with a Pt ultra microelectrode as a WE, a Pt foil as a CE and a saturation calomel electrode (SCE) as a RE to investigate E_{eq} of the iodide/triiodide couple [21]. E_{eq} was found to be stable for the electrolyte with any pyridine derivative indicating the anodic peak potential shift does not arise from the E_{eq} change of iodide/triiodide couple. On the other hand, the shift may result from the different reaction dynamics between the oxidized dye and iodide ion. In the electrolyte with 0.1 mol L^{-1} different pyridine derivatives, the reaction between the oxidized dye and iodide

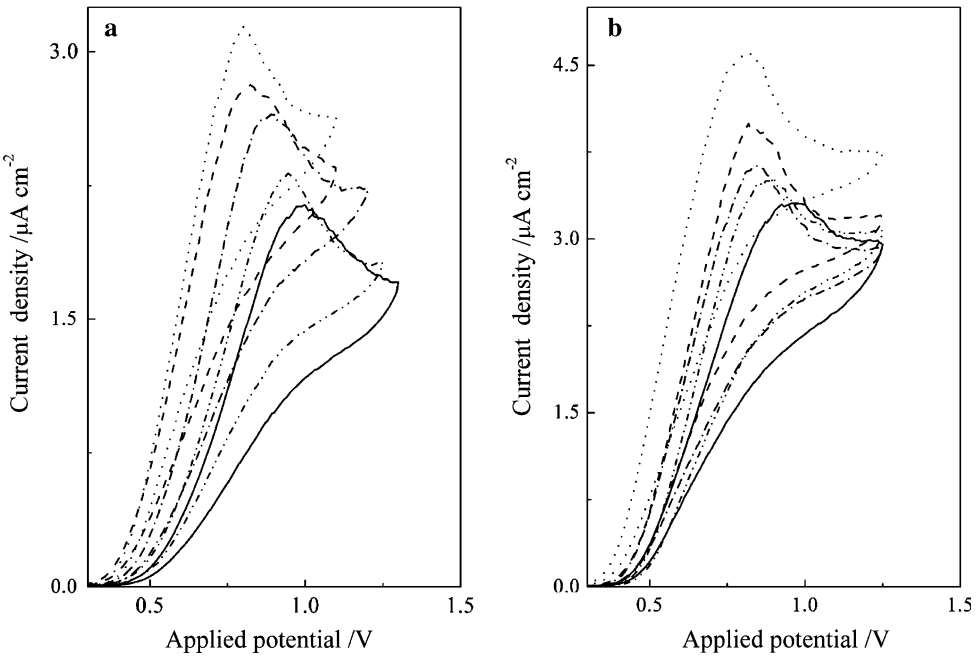

Fig. 2 Cycle voltammograms for the dye coated FTO electrode in blank electrolyte with different concentrations of POP (**a**): 0.1 mol L^{-1} (*dot line*), 0.3 mol L^{-1} (*dash line*), 0.6 mol L^{-1} (*dash-dot line*), 0.8 mol L^{-1} (*dash-dot-dot line*) and 1.0 mol L^{-1} (*solid line*), and in blank electrolyte (*dot line*) with 0.1 mol L^{-1} different additives (**b**): TBP (*dash line*), POP (*dash-dot line*), EOP (*dash-dot-dot line*), *iso*POP (*solid line*)

ion becomes difficult. The same phenomena were also observed with increasing concentration of POP as shown in Fig. 2a. Clifford et al. [22] investigated the regeneration dynamics of N3 in iodide/triiodide electrolyte and revealed that the regeneration reaction proceeds via a transient intermediate complex $[dye^+ \cdot I^-]$ formed by the reaction of the photogenerated dye cation with one iodide ion. Furthermore, Nour-Mohammadi et al. [23] studied the photo substitution reaction between N719 dye and TBP. One of the five degradation products, Ru(H_2dcbpy)(Hdcbpy)(NCS)(TBP), was identified. It is clear that the oxidized dye can react not only with pyridine derivatives but also with iodide ion. In the *CV* measurements, as the applied potential was scanned positively, the dye coated on the FTO WE electrode was oxidized. In the presence of POP at the FTO/dye/electrolyte interface the possible reactions can be summarized as follows

$$Dye - e \rightarrow Dye^+ \quad (1)$$

$$Dye^+ + I^- \rightarrow [Dye^+ \cdot I^-] \quad (2)$$

$$Dye^+ + POP \rightarrow [Dye^+ \cdot POP]. \quad (3)$$

Reactions 2 and 3 have the same dynamic features and are competitive with each other. Reaction 3 decreases the dye cation concentration, which suppresses Reaction 2. With increase in the concentration of POP, Reaction 2 may become increasingly difficult. Consequently, the anodic peak current density decreases and the peak potential shifts positively. For the electrolyte containing 0.1 mol L^{-1} pyridine derivatives, the differences in anodic peak current density and position may result from their abilities to react with the oxidized dye arising from pyridine derivative coordination with ruthenium (II) [24]. The positive shift of anodic peak potential and the decrease in peak current density indicate the slower dye regeneration rate in the electrolyte. This leads to the decay of J_{sc} of DSSCs with the addition of pyridine derivatives.

3.3 Electrochemical impedance spectroscopy for the electrolyte containing pyridine derivatives

During the mediator regeneration cycle in DSSCs, the oxidized species (triiodide) must be reduced to iodide on the counter electrode according to the following reaction

$$I_3^- + 2e \rightarrow 3I^-. \quad (4)$$

In order to compare this reaction rate on the Pt counter electrode after addition of pyridine derivatives, the charge transfer resistance at the Pt/electrolyte interface was determined by EIS [18, 25]. Figure 3 shows typical impedance spectra measured with sandwich type cells (shown in Fig. 4a) consisting of two identical platinized electrodes and electrolyte containing different POP concentration. The equivalent circuit for this type of cell is shown in Fig. 4b. The ohmic series resistance (R_S) representing the resistances of the platinized counter electrode and the electrolyte can be determined according to the high frequency (around 1 MHz) of EIS where the phase is zero. In the middle frequency range 10–1 MHz, the impedance was dominated by the RC network of the Pt electrode and the electrolyte interface, consisting of the charge transfer resistance (R_{CT}) and the capacitance of the electrical double layer (C_{DL}). The impedance at low frequency can be interpreted as Nernst diffusion impedance (Z_N) in the range 1–10 Hz.

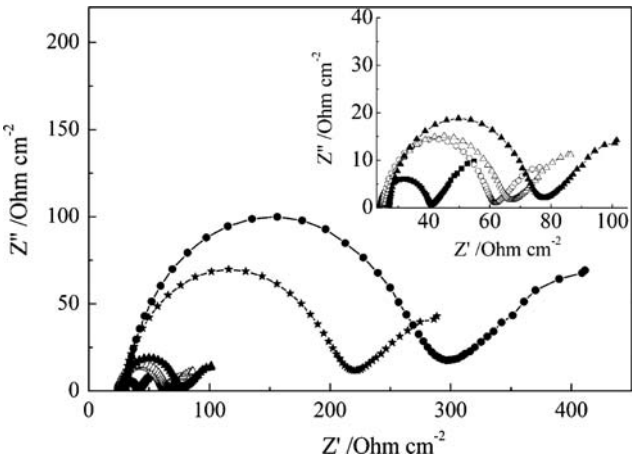

Fig. 3 Electrochemical impedance spectra measured at zero bias under the frequency 0.05 Hz to 1 MHz for a thin-layer cell consisted of two platinized FTO electrodes and blank electrolytes (*filled square*) with different concentrations of POP: 0.1 mol L^{-1} (*open circle*), 0.3 mol L^{-1} (*open triangle*), 0.6 mol L^{-1} (*filled triangle*), 0.8 mol L^{-1} (*filled star*), 1.0 mol L^{-1} (*filled circle*). Inset represents enlargement of the area for Z′ smaller than 100 Ohm cm^{-2}

The R_{ct} values for cells based on blank electrolyte containing different POP concentrations or 0.1 mol L^{-1} different pyridine derivatives were evaluated from the impedance measurement using the equivalent circuit as shown in Fig. 4b and are summarized in Table 2. R_{ct} increases drastically from 1.02 to 14.47 Ω cm^{-2} with POP concentration variation from 0 to 1.0 mol L^{-1} in the electrolyte. Adding different pyridine derivatives to the electrolyte also increases R_{ct} in the following sequence: Blank < TBP < POP < EOP < *iso*POP. R_{ct} represents the resistance related to electron transfer in the reduction of triiodide. As a consequence, increase in R_{ct} implies decay of the triiodide reduction rate and this leads to a decrease in J_{sc} [15].

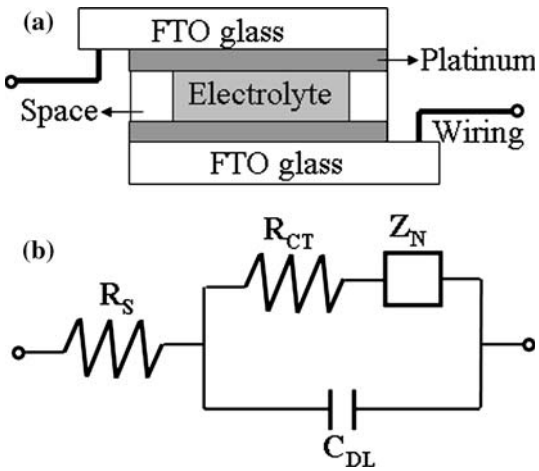

Fig. 4 Schematic structure of cell used in EIS measurements (**a**) and equivalent circuit for EIS (**b**). Z_N: Nernst diffusion impedance; R_{CT}: charge transfer resistance; C_{DL}: capacitance of electrical double layer; R_S: ohmic serial resistance

3.4 UV–Vis spectra analysis

In order to study the effect of pyridine derivatives on R_{ct}, UV–Vis spectra were determined to investigate the interaction between iodine and pyridine derivatives. The molecular structure of pyridine derivatives is shown in Scheme 1. The different derivatives with similar structure have different substitute groups in the 4 position. We choose POP as a basic model compound. Figure 5 shows the absorption spectra of various compounds in MPN at room temperature. The mixture solution without iodine (shown as light gray line) show no absorption peak in the region from 280 to 800 nm whereas 0.1 mol L^{-1} iodine solution shows an absorption at 455 nm. Absorption of

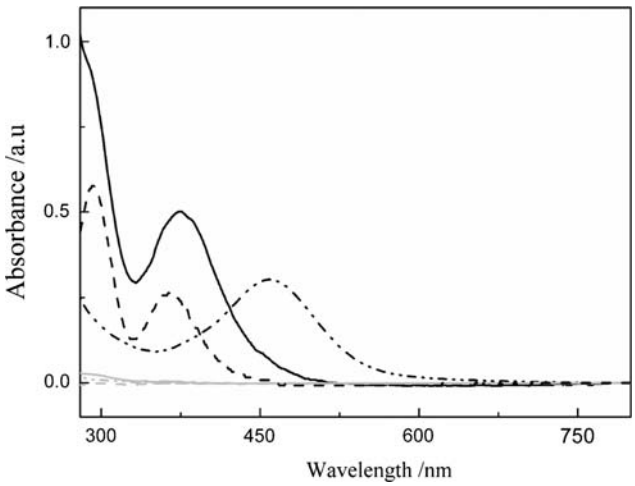

Fig. 5 UV–Vis spectra of solutions with different compounds in MPN at room temperature. 0.1 mol L^{-1} I_2 (*black dash-dot-dot line*), 0.1 mol L^{-1} I_2 + 0.1 mol L^{-1} POP (*black solid line*), 0.1 mol L^{-1} POP (*light gray dash-dot-dot line*), 0.1 mol L^{-1} LiI (*light gray dash line*), 0.1 mol L^{-1} LiI + 0.1 mol L^{-1} POP (*light gray solid line*), 0.1 mol L^{-1} LiI + 0.1 mol L^{-1} I_2 (*black dash line*)

Table 2 Charge transfer resistance (R_{ct}) for different electrolytes

Additive	Blank	0.1 mol L^{-1} TBP	0.1 mol L^{-1} EOP	0.1 mol L^{-1} *iso*POP	0.1 mol L^{-1} POP	0.3 mol L^{-1} POP	0.6 mol L^{-1} POP	0.8 mol L^{-1} POP	1.0 mol L^{-1} POP
R_{ct} (Ω cm^{-2})	1.02	1.54	2.03	2.17	1.81	2.25	2.77	10.51	14.47

0.1 mol L^{-1} LiI/I_2 mixture solution were detected at 291 and 373 nm, which are the characteristic peaks of the triiodide ion [26]. The disappearance of the peak at 455 nm indicates that the iodine was completely converted to triiodide with iodide. However, the mixture of POP and iodine in MPN gives a very intense peak around 378 nm, the absorption of a charge transfer complex between POP and iodine, being different from the absorption of triiodide or iodine in MPN. We interpret the obvious shift of iodine absorption peak from 455 to 378 nm as a consequence of the complex $[POP \cdot I_2]$ formation. This result is in good agreement with literature data reported earlier [27, 28]. If POP reacts in a similar way the following reaction can occur in DSSCs

$$POP + I_3^- \rightarrow POPI_2 + I^-. \quad (5)$$

Reaction 5 leads to a decrease in the triiodide concentration and an increase in the iodide concentration, which enhances the R_{ct} value and decreases the triiodide reduction rate on platinum. This agrees well with the result reported by Nazmutdinova et al. [29]. The formation of a charge transfer complex results in an increase in R_{ct}, and a consequent decay in J_{sc}.

3.5 Photovoltaic performances of DSSCs with pyridine derivatives

Table 3 shows the photovoltaic performances of DSSCs with different POP concentration or 0.1 mol L^{-1} different pyridine derivatives. The conversion efficiency (η) of DSSCs is enhanced after the addition of derivatives as compared to the cell with blank electrolyte. The enhanced solar cell performance is due to the adsorption of derivative at the dye free TiO_2 surface resulting in the suppression of back electron transfer from the TiO_2 conduction band to the triiodide in the electrolyte. Adsorption of pyridine derivatives at the TiO_2 surface is caused by the interaction between the Ti(IV) ion, which is a Lewis acid, and the lone electron pair of pyridine derivatives [3, 12]. The adsorption causes a negative shift of Fermi level of the TiO_2 electrode due to the accumulation of photogenerated electrons in the conduction band. This results in a larger V_{oc} and decreases the driving force for injection of electrons from the LUMO of N3 dye into the conduction band of TiO_2 leading to a decay of J_{sc}. Compared with the blank electrolyte, V_{oc} increases after addition of the pyridine derivatives and J_{sc} falls with increasing POP concentration as shown in Table 3. J_{sc} for cells based on electrolyte with different concentration of POP follows the order: Blank > 0.1 mol L^{-1} > 0.3 mol L^{-1} > 0.6 mol L^{-1} > 0.8 mol L^{-1} > 1.0 mol L^{-1}; and for J_{sc} of 0.1 mol L^{-1} different derivatives as Blank > TBP > POP > EOP > *iso*POP, which is in good agreement with the values of R_{ct} and the anodic peak current.

Table 3 Photovoltaic performances of DSSCs with different POP concentrations or 0.1 mol L^{-1} different additives in blank electrolyte under 100 mW cm^{-2} light irradiation

Electrolyte	V_{oc}(V)	J_{sc}(mA cm^{-2})	*FF*	ŋ(%)
Blank	0.441	18.85	0.45	3.74
0.1 mol L^{-1} POP	0.642	14.50	0.66	6.14
0.3 mol L^{-1} POP	0.657	11.25	0.64	4.73
0.6 mol L^{-1} POP	0.682	11.00	0.65	4.88
0.8 mol L^{-1} POP	0.695	10.80	0.62	4.65
1.0 mol L^{-1} POP	0.703	10.65	0.63	4.72
0.1 mol L^{-1} TBP	0.603	16.55	0.61	6.09
0.1 mol L^{-1} EOP	0.638	13.85	0.62	5.48
0.1 mol L^{-1} *iso*POP	0.643	13.55	0.60	5.23

4 Conclusions

New kinds of pyridine derivatives were synthesized and their electrochemical behavior as additives in the electrolyte of DSSCs was investigated using cyclic voltammetry and electrochemical impedance measurements. With addition of derivatives, a complex between triiodide ion and the pyridine derivative is formed as identified by the strong absorption at 378 nm. Competitive reactions of the oxidized dye with pyridine derivative and the iodide lead to a decrease in the dye regeneration rate as studied by means of the flash photolysis analysis. After the addition of pyridine derivative two processes of dye regeneration reaction at the nanocrytalline TiO_2 electrode and triiodide reduction at the platinum counter electrode become slower. This leads to a decay of J_{sc}.

Acknowledgments This work was supported by the National Research Fund for Fundamental Key Project (2006CB202605) and the National Natural Science Foundation of China (50221201 and 50473055). Thanks to Qiqiang Wang and Min Liu for the help towards the synthesis. Experimental help from Shujing Feng and Hanping Zhang are gratefully acknowledged.

References

1. O'Regan B, Grätzel M (1991) Nature 353:737
2. Nazeeruddin MK, Kay A, Rodicio I, Humphry-Baker R, Muller E, Liska P, Valchopoulos N, Grätzel M (1993) J Am Chem Soc 115:6382
3. Grätzel M (2001) Nature 414:338
4. Palomares E, Clifford JN, Haque SA, Lutz T, Durrent JR (2003) J Am Chem Soc 125:475
5. Schlichthörl G, Huang SY, Sprague J, Frank AJ (1997) J Phys Chem B 101:8141
6. Hong JS, Joo M, Vittal R, Kim KJ (2002) J Electrochem Soc 149:E493

7. Neal NR, Kopidakis N, Lagemant J, Grätzel M, Frank AJ (2005) J Phys Chem B 109:23183
8. Nakade S, Kanzaki T, Kubo W, Kitamura T, Wada Y, Yanagida S (2005) J Phys Chem B 109:3480
9. Zhang Z, Evans N, Zakeeruddin SM, Humphry-Baker R, Grätzel M (2007) J Phys Chem C 111:398
10. Kusama H, Sugihara H (2006) Sol Energy Mater Sol Cells 90:953
11. Wang M, Zhang QL, Weng YX, Lin Y, Xiao XR (2006) Chin Phys Lett 23:724
12. Yin X, Zhao H, Cheng LP, Tan WW, Zhang JB, Weng YX, Shuai ZG, Xiao XR, Zhou XW, Li XP, Lin Y (2007) Surf Interface Anal 39:809
13. Wang GQ, Lin Y, Xiao XR, Li XP, Wang WB (2004) Surf Interface Anal 36:1437
14. Wang M, Xiao XR, Zhou XW, Li XP, Lin Y (2007) Sol Energy Mater Sol Cells 91:785
15. Wang GQ, Zhou XW, Li MY, Zhang JB, Kang JJ, Lin Y, Fang SB, Xiao XR (2004) Mater Res Bull 39:2113
16. Gan Q, Li SY, Morlet-Savary F, Wang SQ SQ, Shen S, Xu HJ, Yang GQ (2005) Opt Express 13:5424
17. Zhang CX, Liang HC, Kim E-i , Shearer J, Helton ME, Kim E, Kaderli S, Incarvito CD, Zuberbühler AD, Rheingold AL, Karlin KD (2003) J Am Chem Soc 125:634
18. Hom RK, Chi DY, Katzenellenbogen JA (1996) J Org Chem 61:2624
19. Zhang CX, Kaderli S, Costas M, Kim E-i , Neuhold YM, Karlin KD, Zuberbühler AD (2003) Inorg Chem 42:1807
20. Nogueira AF, De Paoli MA, Montanari I, Monkhouse R, Nelson J, Durrant JR (2001) J Phys Chem B105:751
21. Wang P, Zakeerudin SM, Comte P, Exnar I, Grätzel M (2003) J Am Chem Soc 125:1166
22. Clifford JN, Palomares E, Nazeruddin K, Grätzel M, Durrant JR (2007) J Phys Chem C 111:6561
23. Nour-Monammadi F, Nguyen HT, Boschloo G, Lund T (2007) J Photochem Photobiol A Chem 187:348
24. Chen H, Li Z, Ye H, Wang M (2004) Mater Sci Eng B 111:242
25. Hauch A, Geory A (2001) Electrochim Acta 46:3457
26. Popov AI, Skelly NE (1995) J Am Chem Soc 77:3722
27. Kebede Z, Lindquist S-E (1999) Sol Energy Mater Sol Cells 57:259
28. Tassaing T, Besnard M (1997) J Phys Chem A 101:2803
29. Nazmutdinova G, Sensfuss S, Schrödner M, Hinsch A, Sastrawan R, Gerhard D, Himmler S, Wasserscheid P (2006) Solid state Ion 177:3141